The expansion of MDSCs induced by exosomal PD-L1 promotes the progression of gastric cancer

Huaizhi Li[1,2†], Xu Chen[1,2†], Shanshan Zheng[1,2†], Bo Han[1,2], Xiang Zhang[1,2], Xiaoxia Zheng[1,2], Yujia Lu[1,2], Qingmin Sun[1], Xufeng Hu[3*] and Jian Wu[1*]

Abstract

Background Myeloid-derived suppressor cells (MDSCs) are the major factor in gastric cancer (GC) immune evasion. Nevertheless, the molecular process underlying the expansion of MDSCs induced by tumor-derived exosomes (TDEs) remains elusive.

Methods The levels of exosomal and soluble PD-L1 in ninety GC patients were examined via enzyme-linked immunosorbent assay (ELISA) to determine their prognostic value. To investigate the correlation between exosomal PD-L1 and MDSCs, the percentage of MDSCs in the peripheral blood of 57 GC patients was assessed via flow cytometry. Through ultracentrifugation, the exosomes were separated from the GC cell supernatant and detected via Western blotting, nanoparticle tracking analysis (NTA), and transmission electron microscopy (TEM). The function of exosomal PD-L1 in MDSCs was evaluated via immunofluorescence, Western blotting and flow cytometry in a GC cell-derived xenograft (CDX) model.

Results The overall survival (OS) of GC patients in the high exosomal PD-L1 group was significantly lower than that of patients in the low exosomal PD-L1 group ($P = 0.0042$); however, there was no significant correlation between soluble PD-L1 and OS in GC patients ($P = 0.0501$). Furthermore, we found that the expression of exosomal PD-L1 was positively correlated with the proportions of polymorphonuclear MDSCs (PMN-MDSCs, $r = 0.4944$, $P < 0.001$) and monocytic MDSCs (M-MDSCs, $r = 0.3663$, $P = 0.005$) in GC patients, indicating that exosomal PD-L1 might induce immune suppression by promoting the aggregation of MDSCs. In addition, we found that exosomal PD-L1 might stimulate MDSC proliferation by triggering the IL-6/STAT3 signaling pathway in vitro. The CDX model confirmed that exosomal PD-L1 could stimulate tumor development and MDSC amplification.

---

†Huaizhi Li, Xu Chen and Shanshan Zheng contributed equally to this work.

*Correspondence:
Xufeng Hu
15961506615@163.com
Jian Wu
jianwu@njucm.edu.cn

Full list of author information is available at the end of the article

Li *et al. Journal of Translational Medicine*   (2024) 22:821

Page 2 of 15

Conclusions Exosomal PD-L1 has the potential to become a prognostic and diagnostic biomarker for GC patients. Mechanistically, MDSCs can be activated by exosomal PD-L1 through IL-6/STAT3 signaling and provide a new strategy against GC through the use of exosomal PD-L1 as a treatment target.

Keywords PD-L1, Exosomes, MDSCs, Gastric cancer

Introduction

Gastric cancer (GC) ranks fourth in the world in terms of cancer-related deaths and is the fifth most common type of cancer worldwide [1]. The 5-year relative survival rate for GC patients remains remarkably low (20–30%) [2]. Surgery followed by adjuvant chemotherapy or chemoradiotherapy is the standard-of-care treatment for half of GC patients who are eligible for surgery [3, 4]. Glutamic acid and its derivatives glutamine, antifungal drugs, thalidomide and its derivatives, and nanocarrier drugs have good anticancer effects on some cancer cells [5–9]. In the preclinical model, combined blocking of PD-L1 and IL-6 receptor (IL6R) can synergistically regress the established large tumors and significantly improve the antitumor CD8$^+$cytotoxic T lymphocyte (CTL) response compared with the use of anti-PD-L1 alone, and IL-6-STAT3 signaling inhibited the classical cytotoxic differentiation of CTLs in vitro [10]. The activation of IL-6/STAT3 signaling can also lead to GC cells growth and migration [11, 12].

The tumor microenvironment (TME) is a highly structured ecosystem that contains cancer cells, immune cells, cancer-associated fibroblasts (CAFs), endothelial cells (ECs), pericytes, and other cell types. It is associated with maintaining proliferation signaling, resisting cell death, inducing angiogenesis, activating invasion and metastasis, triggering proinflammatory cytokines, and preventing immune damage in cancer [13–15]. The TME of GC is a complex system that can inhibit the immune response and promote tumor progression, which is largely affected by the matrix components. Tumor cells can mobilize these matrix components to inhibit multiple steps of T cell activation, leading to immunosuppression [16]. MDSC is the main immunosuppressive cell in TME. Elevated PD-L1 expression in the gastric epithelium can increase the number of MDSCs infiltrating tumors, and the levels of chemokines and cytokines are related to the migration, differentiation, recruitment and immune activity of MDSCs [17].

Exosomes are structures with an average size of 100 nm that can transport proteins, lipids, and nucleic acids, which are able to modulate components of the tumor microenvironment and influence the proliferation and migration rates of cancer cells [18]. Notably, exosomes are present in different body fluids, such as blood circulation, and can be employed as biomarkers for the diagnosis of diabetic patients [19, 20]. Tumor-derived exosomes (TDEs) have recently been demonstrated to impact noncancerous cells, creating a tumor microenvironment that supports tumor growth and metastasis [21]. TDEs released into the extracellular milieu and circulation contain the PD-L1 protein [22, 23]. Exosomal PD-L1 is considered to be a useful predictor in anti-PD-1 therapy [24] and has the ability to prevent T cells from destroying breast cancer cells and promote tumor growth [25]. However, the biological mechanism by which exosomal PD-L1 induces immunosuppression during the progression of GC remains unclear.

In our exploration of PD-L1 function in the TME of GC, we compared soluble PD-L1, and PD-L1 is largely enriched in exosomes. Moreover, compared with those of normal individuals, the serum exosomes of GC patients contain higher levels of PD-L1, and higher levels of exosomal PD-L1 are related to poor prognosis in GC patients, suggesting that exosomal PD-L1 might be an applicable prognostic indicator for GC. In addition, we found that circulating exosomal PD-L1 was strongly correlated with the proportion of MDSCs in the peripheral blood of GC patients. In vivo experiments, revealed that exosomal PD-L1 promoted the expansion of MDSCs and the progression of GC. Mechanically, exosomal PD-L1 might activate the IL-6/STAT3 signaling pathway, which increases the number of MDSCs. These results reveal a new mechanism by which PD-L1 promotes the progression of GC and may provide a new strategy for immunotherapy against GC through the use of exosomal PD-L1 as a treatment target.

Materials and methods

Patients and clinical samples

Thirty female and sixty male GC patients who were treated at the Affiliated Hospital of Nanjing University of Chinese Medicine between 2018 and 2022 were included in this study. In addition, 72 physically fit individuals were chosen for this study's typical control group. Table 1 provides all of the patients' clinical data, which included their vital status, age, gender, pTNM stage, tumor size, lymph node metastases, vascular invasion, and chemotherapy conditions. All patients provided the informed permission, and the Ethics Committee of the Affiliated Hospital of Nanjing University of Chinese Medicine approved this study, which was carried out in accordance with the Declaration of Helsinki's principles (2021NL-133-03).
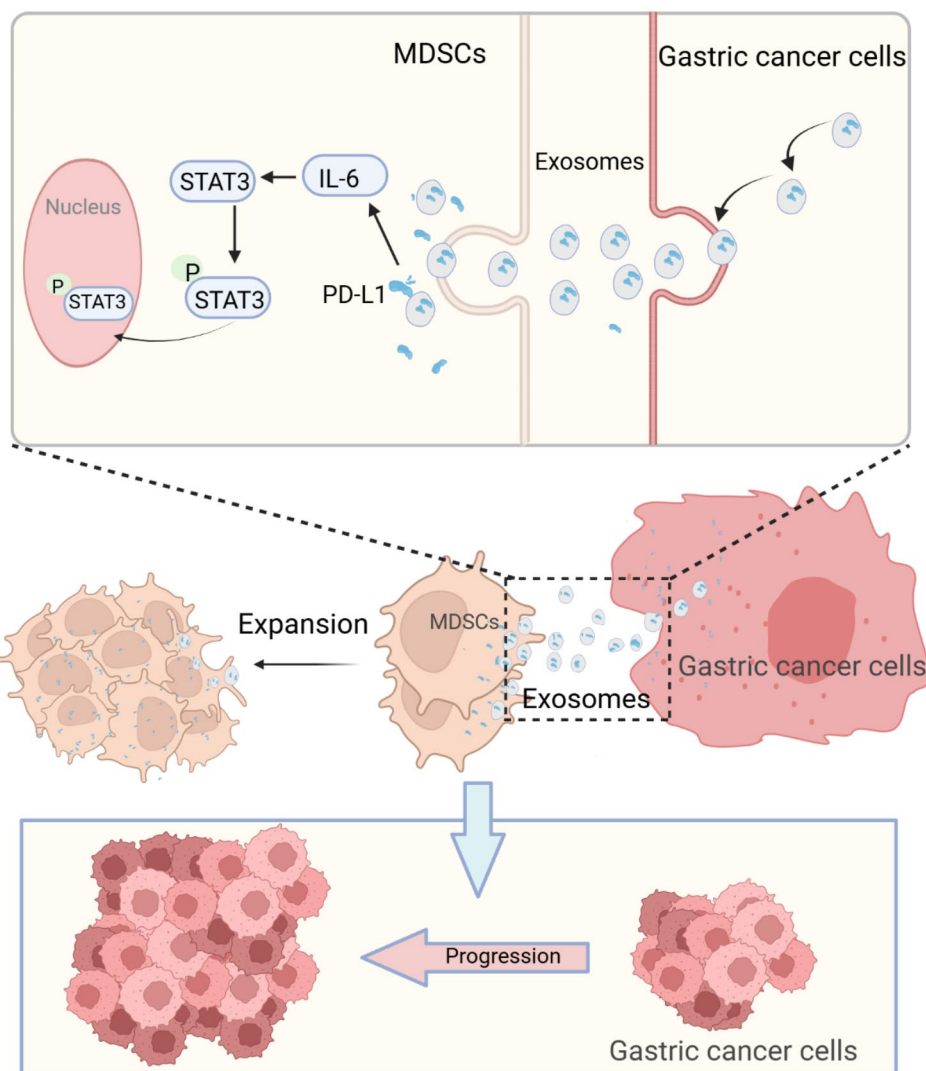
Schematic illustration depicting the intrinsic relationship between GC cells and MDSCs in the tumor microenvironment

Cell lines and cell culture

MFCs, murine GC cell lines, were purchased from the Cell Bank of the Chinese Academy of Sciences (Shanghai, China). The cells were cultured at 37 °C and 5% CO_2 in RPMI 1640 (Gibco, Grand Island, United States) medium supplemented with 10% fetal bovine serum (FBS) (Ever-green Company, China). The cells were subcultured or the media was replaced when they had grown to a conflu-ence of 80–90%.

MDSCs are produced by bone marrow (BM) progenitor cells

In accordance with earlier techniques, BM cells were isolated [26]. Briefly, BM cells were obtained from the femurs and tibias of male C57BL/6 mice (18–22 g, 6 weeks old; purchased from Tianjin Institute of Hema-tology). A 70 µm cell filter was used to filter the cell suspension. Red blood cell lysis buffer (Beyotime, C3702) was incubated at room temperature for 4 min after the isolated cells were centrifuged at 4 °C for 6 min (600 × g). Subsequently, PBS was used to terminate the process of lysis, and the cells were collected. After that, the BM cells were plated at a density of 5×10^5 cells/mL in 6-well plates. On the basis of an earlier in vitro investigation, 100 µg/mL exosomes were chosen for further induction [26, 27]. The granulocyte and macrophage colony-stim-ulating factor (GM-CSF, 20 ng/mL) (Peprotech, 031955), 10% FBS supplied without exosomes, and RPMI 1640 medium were used to cultivate the BM cells. Exosomes (100 µg/mL) were subsequently added for intervention. Using flow cytometry, the cell phenotype was identified following 4 days of incubation.

Li *et al. Journal of Translational Medicine*   (2024) 22:821

Page 4 of 15

Table 1 Characteristics of GC patients

Characteristics	Variable	Patients (90)	Percentages (%)
Vital status			
	Alive	42	46.67
	Death	48	53.33
Age (years)			
	≤60	36	40
	>60	54	60
Gender			
	male	60	66.67
	female	30	33.33
Lauren classification			
	Intestinal	22	24.44
	Diffuse and mixed	58	64.44
	Not stated	10	11.11
Tumor size (cm)			
	>3	56	62.22
	<3	34	37.78
Lymph node metastasis			
	N0	36	40
	N1-N3	53	58.89
	Not stated	1	1.11
pTNM stage			
	I and II	49	54.44
	III and IV	41	45.56
vascular invasion			
	yes	38	42.22
	No	51	56.67
	Not stated	1	1.11
Chemotherapy			
	sensitive	46	51.11
	resistant	22	24.44
	no chemotherapy	22	24.44

Lentivirus generation and transfection

The PD-L1 sequence was amplified from the full-length cDNA of mice by Shanghai GeneChem Company and subcloned and inserted into the GV493 vector. The vector element was hU6-MCS-CBh-gcGFP-IRES-puromycin. The vector was co-transfected into 293T cells via lipo3000 (Thermo) according to the manufacturer's protocol. The PD-L1 shRNA expressing lentivirus was harvested and stored at -80 °C for 3 days. Western blotting experiments revealed that PD-L1 gene expression was sufficiently, downregulated, and the dilution was set to 20 MOI for subsequent experiments.

Isolation and identification of exosomes

Plasma exosomes Firstly, 400 μL plasma samples were centrifuged at 4 °C for 30 min at 10,000 × g to remove cells and their fragments. The ExoQuick (System Biosciences, EXOQ5TM-1) reagent (0.25 volume) was added to

the samples according to the manufacturer's instructions. After incubation at 4 ℃ for 16 h, the mixture of plasma and reagents was centrifuged at 1,500 × g for 30 min to precipitate the exosomes. Finally, 100 μL of PBS was used to resuspend the exosome particles, which were subsequently stored at -80 °C.

Cell culture supernatant The cell culture supernatant was centrifuged at 800 × g for 5 min, 2,000 × g for 10 min, 10,000 × g for 30 min, and 100,000 × g for 80 min. The supernatant was discarded, and the exosome particles were resuspended in PBS and ultracentrifuged at 100,000 × g for 80 min. All the experiments were carried out at 4 °C. The exosomes were subsequently resuspended in PBS and stored at 4 °C (1–7 days) or -80 °C for a long period of time.

Identification Exosomes suspension (20 μL) was placed on copper with no liquid for 3 min, and 2% phosphotungstic acid solution was used to counterstain them for 10 min. The exosomes were dried under an incandescent lamp for 2 min and photographed via transmission electron microscopy (TEM, Tecnai-12; Philips, Netherlands). The size and concentration of the particles were detected via nanoparticle tracking analysis (NTA, Particle Metrix, Germany). The expression of CD9, CD63 and TSG101, makers of exosomes, was examined via western blotting.

ELISA

A human PD-L1 ELISA kit (JiyinmeiBio, JYM1968Hu) was used for quantitation of the PD-L1 in plasma following the manufacturer's instructions. Exosome-bound buffer was used to resuspend exosome particles isolated from plasma for ELISA. The total protein content of the exosomes was determined via a BCA protein analysis kit (Beyotime Biotechnology, Shanghai, China). The content of PD-L1 in exosomes was determined via a human PD-L1 ELISA kit. Specifically, 100 μL exosomes were added to each well and incubated for 2 h. Then, human PD-L1 detection antibody was added to each well and incubated for 2 h. 100 μL of horseradish peroxidase-conjugated streptavidin (streptavidin-HRP) was added to each well in 1% BSA PBS at pH 7.2 ~ 7.4, added (R&D, Catalog # DY995), and incubated for 20 min. Then, 100 μL of a 1 : 1 mixture of Color Reagent A (H2O2) and Color Reagent B (tetramethylbenzidine) (R&D, Catalog # DY999) was added to the substrate solution and incubated at room temperature for 20 min. The reaction was terminated with 2 N H_2SO_4 (R&D, Catalog # DY994). The standard curve was made by human PD-L1 standard. The absorbance was measured at a wavelength of 490 nm via a microplate reader. All operations were performed in strict accordance with the instructions.
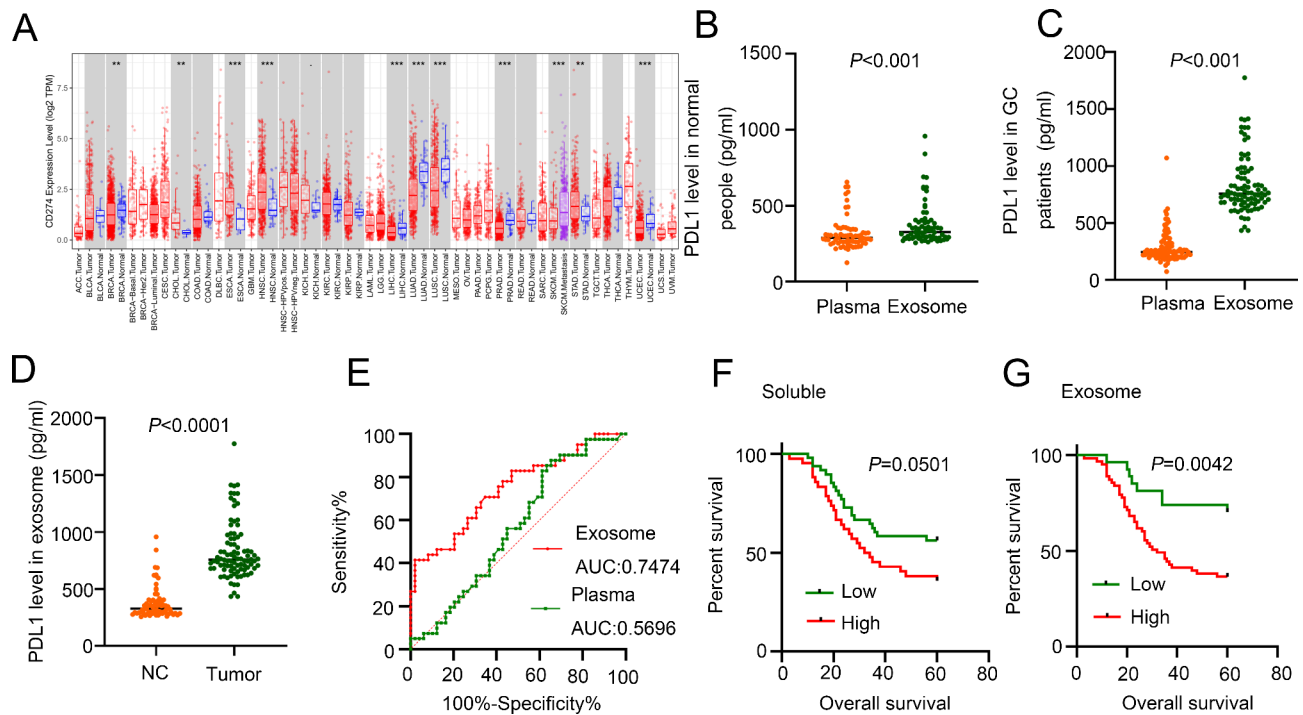
Fig. 1 Exosomal PD-L1 was positively associated with poorer prognosis in GC patients. (**A**) The expression level of PD-L1 (CD274) in different types of tumor tissues and normal tissues in the TIMER database. (**B-C**) The levels of soluble PD-L1 and exosomal PD-L1 in normal individuals and GC patients. (**D**) The levels of exosomal PD-L1 in normal individuals and patients with GC. The significance of the difference was tested with an unpaired t test. (**E**) Receiver operating characteristic (ROC) curve analysis revealed high expression specificity of exosomal PD-L1 in GC patients. AUC, area under the curve. (**F-G**) Kaplan–Meier (KM) survival curve for patients classified as showing either high or low expression of soluble PD-L1 or exosomal PD-L1 in GC according to the ROC curve cutoff value. The significance of the prognostic value was tested by a log-rank test. (*$P < 0.05$, **$P < 0.01$, ***$P < 0.001$)

Flow cytometry

The tumor tissues were washed with ice-cold PBS, and then the tissue was cut into 0.1 mm^3 pieces. The cells were isolated by incubating the tissues with digestion buffers including RPMI 1640, 5% FBS, 1 mg/mL collagenase IV (BioFroxx, 2091MG100), 0.2 mg/mL DNaseI (SigmaAldrich, D2821) and 0.2 mg/mL hyaluronidase (BioFroxx, 1141MG100). The suspension was shaken at 37 °C for 1 h, filtered through a 70 μm cell filter, and centrifuged at $800 \times g$ at 4 °C for 5 min to collect the cells. The single-cell suspensions (1×10^7 cells/mL) obtained as described above were incubated with the fluorescent dye-conjugated antibodies AF488-CD45 (Elabscence, E-AB-F1136L), PE/Dazzle, TM 594-CD11b (BioLegend, 101256) and APC-Gr-1 (BioLegend, 108412) at 4 °C for 30 min. The cells were analyzed via FACSVerse (BD Biosciences, MA). Human MDSCs were isolated by incubating the peripheral blood of GC patients with the fluorescent dye-conjugated antibodies PE-CY7-CD11b (BD Pharmingen, 557743), PE-CD14 (BioLegend, 301806), FITC-CD15 (BioLegend, 323004), and APC-HLA-DR (BioLegend, 307610). The cells were analyzed via a FACSVerse (BD Biosciences, MA) after washing. FlowJo software was used to analyze the results.

Western blotting

The cells and exosomes were lysed via RIPA buffer (Beyotime) containing a protease/phosphatase inhibitor cocktail for 15 min to obtain total protein. A BCA protein assay kit (Beyotime) was used to determine protein concentrations. Thereafter, the proteins were separated via polyacrylamide gel electrophoresis (PAGE) and transferred to polyvinylidene fluoride (PVDF) membranes. The Western blotting steps were carried out in strict accordance with published methods [28]. The membranes were incubated with the primary antibody and placed in a 4 ℃ refrigerator overnight. The following antibodies were used: anti-iNOS (Proteintech, 22226-1-AP, 1:5000), anti-PD-L1 (Proteintech, 66248-1-Ig, 1:3000), anti-Arg-1 (Proteintech, 16001-1-AP, 1:2000), anti-GADPH (Proteintech, 60004-1-Ig, 1:10000), anti-CD9 (Proteintech, 20597-1-AP, 1:2000), anti-CD63 (Proteintech, 25682-1-AP, 1:2000), anti-TSG101 (Proteintech, 28283-1-AP, 1:3000), anti-STAT3 (Proteintech, 10253-2-AP, 1:5000), anti-p-STAT3 (Cell Signaling Technology, 9145 S, 1:1000), and anti-IL-6 (Cell Signaling Technology, 12912 S, 1:1000). The membranes were further incubated with an HRP-labeled secondary antibody (#7074, 1:2000, CST) at room temperature for 1 h. Finally, the protein signal was detected via the enhanced chemiluminescence
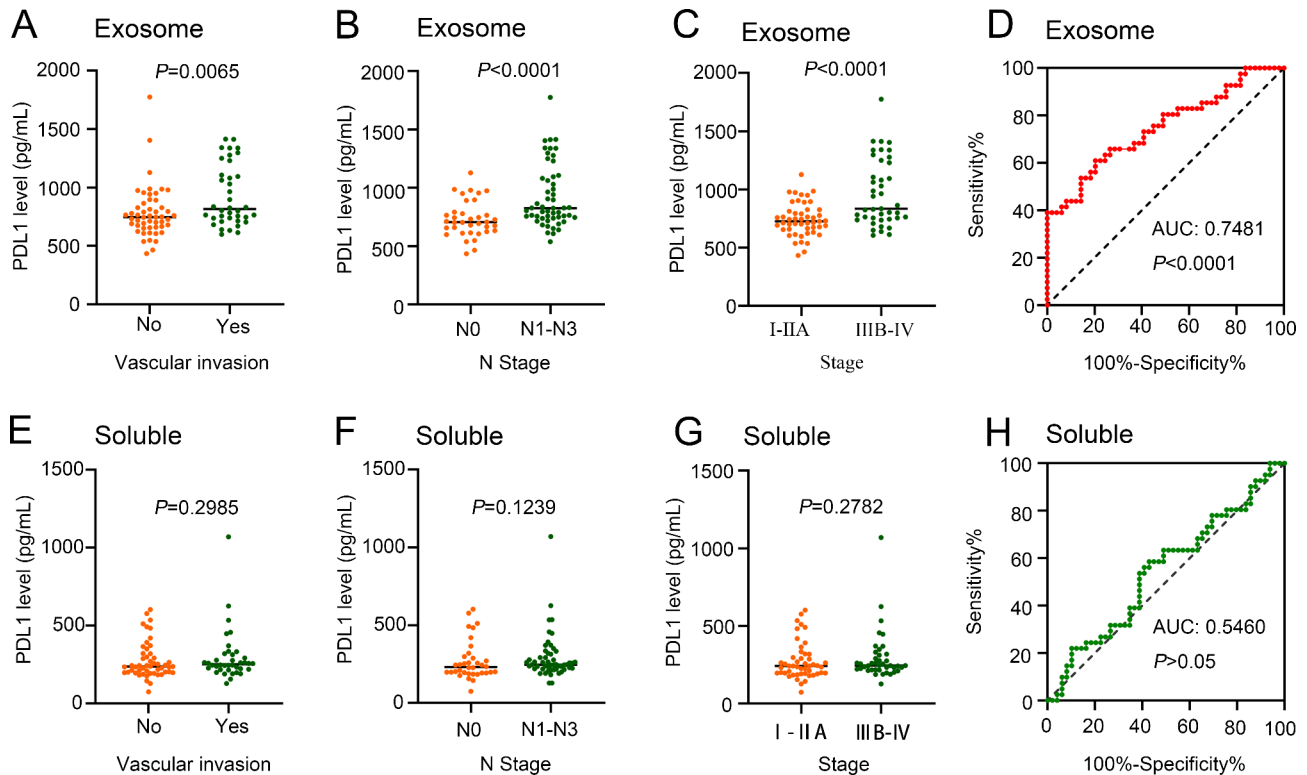
Fig. 2 Associations between exosomal and soluble PD-L1 and the clinicopathological characteristics of patients with GC. (**A-C, E-G**) Correlations between exosomal PD-L1 and soluble PD-L1 and vascular invasion, lymph node metastasis and stage in GC patients. (**D, H**) Receiver operating characteristic (ROC) curve analysis revealed high-expression specificity of exosomal PD-L1 in advanced stage GC. AUC, area under the curve. The significance of the difference was tested with an unpaired t test and one-way ANOVA

(ECL) method. ImageJ software (NIH, Bethesda, MD, United States) was used to quantify the expression level of each protein.

Establishment of a xenograft tumor model

A total of 615 strain mice (male, 6–8 weeks old, weighing 20 ± 1 g) were purchased from Tianjin Institute of Blood. Before the experiment, all the purchased mice were allowed to adapt to the feeding conditions in a pathogen-free environment within one week. For the subcutaneous tumor formation experiments, $5\times10^7/200$ μL MFC cells were digested, resuspended in sterilized PBS, and then injected into the right axilla of each mouse. After the tumor volume reached approximately 100 mm^3, the mice were randomly divided into three groups: the PBS group, PD-L1 Negative Control group (PD-L1-NC-Exo group) and PD-L1 Knock Down group (PD-L1-KD-Exo group), with 6 mice in each group. The mice were treated with PBS, or 20 μg PD-L1-NC or PD-L1-KD exosomes via intratumoral injection two times a week. After 21 days, the mice were euthanized by an overdose of pentobarbital sodium (100 mg/kg i.p.), and the spleen and tumors were isolated and weighed. Animal experiments were performed under specific pathogen-free conditions and protocols were approved by the Experimental Animal

Ethics Committee of Nanjing University of Traditional Chinese Medicine (No. 2021DW-35-01).

Immunofluorescence staining

Tumor tissues from the mice were analyzed via primary antibodies against CD11b (Servicebio, GB11058, 1:5000), anti-Gr-1 (Servicebio, GB11229, 1:5000), and anti-PD-L1 (Servicebio, GB12339, 1:2000). The sections were observed and photographed via a fluorescence microscope.

Statistics

The results were analyzed with GraphPad Prism 8.0 via Student's t test (unpaired, two-tailed) or one-way analysis of variance (ANOVA), followed by Tukey's post hoc tests. The data are expressed as the mean$\pm$SEM of three independent experiments. The overall survival of patients was determined via Kaplan–Meier analysis. The correlation between gene expression was determined via Pearson's correlation analysis. The log-rank test was used for statistical analysis. *$P<0.05$ was considered statistically significant.

Results

Exosomal PD-L1 was associated with poor prognosis in GC patients

First, the Oncomine database was used to evaluate the expression of PD-L1 in various tumor and normal tissue types. The results revealed that PD-L1 was highly expressed in a number of cancer types, such as head and neck squamous cell carcinoma (HNSC), breast invasive carcinoma (BRCA), cholangio carcinoma (CHOL), esophageal carcinoma (ESCA), kidney chromophobe (KICH), and stomach adenocarcinoma (STAD) (Fig. 1A), suggesting that PD-L1 was crucial for the emergence of several tumor types. Additionally, we quantified the levels of soluble and exosomal PD-L1 in the peripheral blood of GC patients and normal individuals. The clinical characteristics of the 90 GC patients are summarized in Table 1. The results revealed that exosomes contained a large amount of PD-L1 (Fig. 1B-C), and compared with normal individuals, GC patients presented a much greater level of enrichment of exosomal PD-L1 (Fig. 1D). The expression specificity of soluble and exosomal PD-L1 was evaluated via a receiver-operating characteristic (ROC) curves in GC patients. Exosomal PD-L1 displayed an area under the curve (AUC) of up to 0.7474, which was greater than that of soluble PD-L1 (0.5696, Fig. 1E). Finally, Kaplan-Meier model analysis was carried out to examine the correlation between soluble and exosomal PD-L1 and the prognosis of patients with GC. However, soluble PD-L1 did not significantly predict the survival of GC patients (Fig. 1F). Notably, overall survival was considerably shorter in patients with higher exosomal PD-L1 levels than in those with lower exosomal PD-L1 levels ($P=0.0042$, Fig. 1G). These results suggested that exosomal PD-L1, rather than soluble PD-L1, was significantly associated with poor prognosis in patients with GC.

Exosomal PD-L1 can be used to distinguish the clinicopathological characteristics of GC patients

A comparison analysis was carried out using patients with various stages of GC. We observed significantly higher levels of exosomal PD-L1 in patients with vascular invasion, lymph node metastasis or advanced-stage disease (stage III/IV) than in patients with no vascular invasion, without lymph node metastasis or with early-stage disease (stage I/II) ($P<0.01$, $P<0.001$ and $P<0.0001$; Fig. 2A–C), respectively. Significant correlations between soluble PD-L1 and these parameters were not detected (Fig. 2E-G). In addition, we did not detect any significant correlations between the levels of exosomal and soluble PD-L1 and other parameters (Fig. S1A–J). ROC curve analysis was performed to evaluate the ability of exosomal PD-L1 and soluble PD-L1 to predict the early or advanced stage of GC. As expected, the AUC of the

exosomal PD-L1 group reached 0.7481 (Fig. 2D), which was greater than that of the soluble PD-L1 group (0.5460, Fig. 2H). Overall, these results showed that GC patients with varying levels of exosomal PD-L1 presented distinct patterns of clinical and pathological characteristics. Exosomal PD-L1 was explicitly enriched in the advanced stage (stage III/IV) and may function as a potential malignancy biomarker of GC.

Exosomal PD-L1 was significantly associated with the aggregation of MDSCs in GC patients

To investigate the key factors that exosomal PD-L1 affected the progress of GC patients, we extracted MDSCs from the peripheral blood of GC patients (Fig. 3A). MDSCs were divided into polymorphonuclear (PMN-MDSCs, $CD11b^+CD14^-CD15^+$) and monocytic (M-MDSCs, $CD11b^+CD14^+HLA-DR^{low}$) (Fig. 3A). As expected, the level of exosomal PD-L1 was similar to those for frequencies of PMN-MDSCs ($r=0.4944$, $P<0.0001$; Fig. 3B) and M-MDSCs ($r=0.3663$, $P=0.005$; Fig. 3C) in the peripheral blood of GC patients. Furthermore, negative correlation was found between patient OS and the proportion of PMN-MDSCs ($P=0.02$, Fig. 3D), but not M-MDSCs ($P=0.08$, Fig. 3E). In addition, integrated tumor-immune system interaction storage portal (TISIDB) network server and tumor immune estimation resource (TIMER) were used to evaluate the correlation between PD-L1 and MDSCs in tumor microenvironment. The correlation between PD-L1 and CD11b (a marker of MDSCs), MDSCs, B cells, NK cells, Treg cells, Th1, Th2, Th17 cell and macrophage was analyzed (Fig. 3F), indicating PD-L1 had a strong correlation with MDSCs ($r=0.59$, $P<0.0001$) and CD11b ($r=0.47$, $P<0.001$; Fig. 3G) in STAD, which was consistent with the above results. These results suggested that the exosomal PD-L1 was highly associated with MDSCs, which might be a main reason of leading to poor prognosis in GC patients.

Exosomes promoted the proliferation of MDSCs and enhanced its immunosuppressive properties in vitro

To determine the effect of GC-derived exosomes on MDSCs, we further extracted exosomes from the supernatant of the GC cells. Exosomes are 40–150 nm extracellular vesicles with double membranes and are positive with CD9, CD63 and TSG101 (Fig. 4A-C). Next, in order to observe the effect of exosomes on MDCSs, BM cells were extracted from C57BL/6J male mice. A certain proportion of BM cells in mice have the phenotype of MDSCs [29], which can be generated from BM progenitors as described previously [26]. To investigate whether GC-derived exosomes could stimulate MDSCs ($CD11b^+Gr-1^+$) expansion, BM-derived MDSCs were cultured with exosomes derived from supernatants of
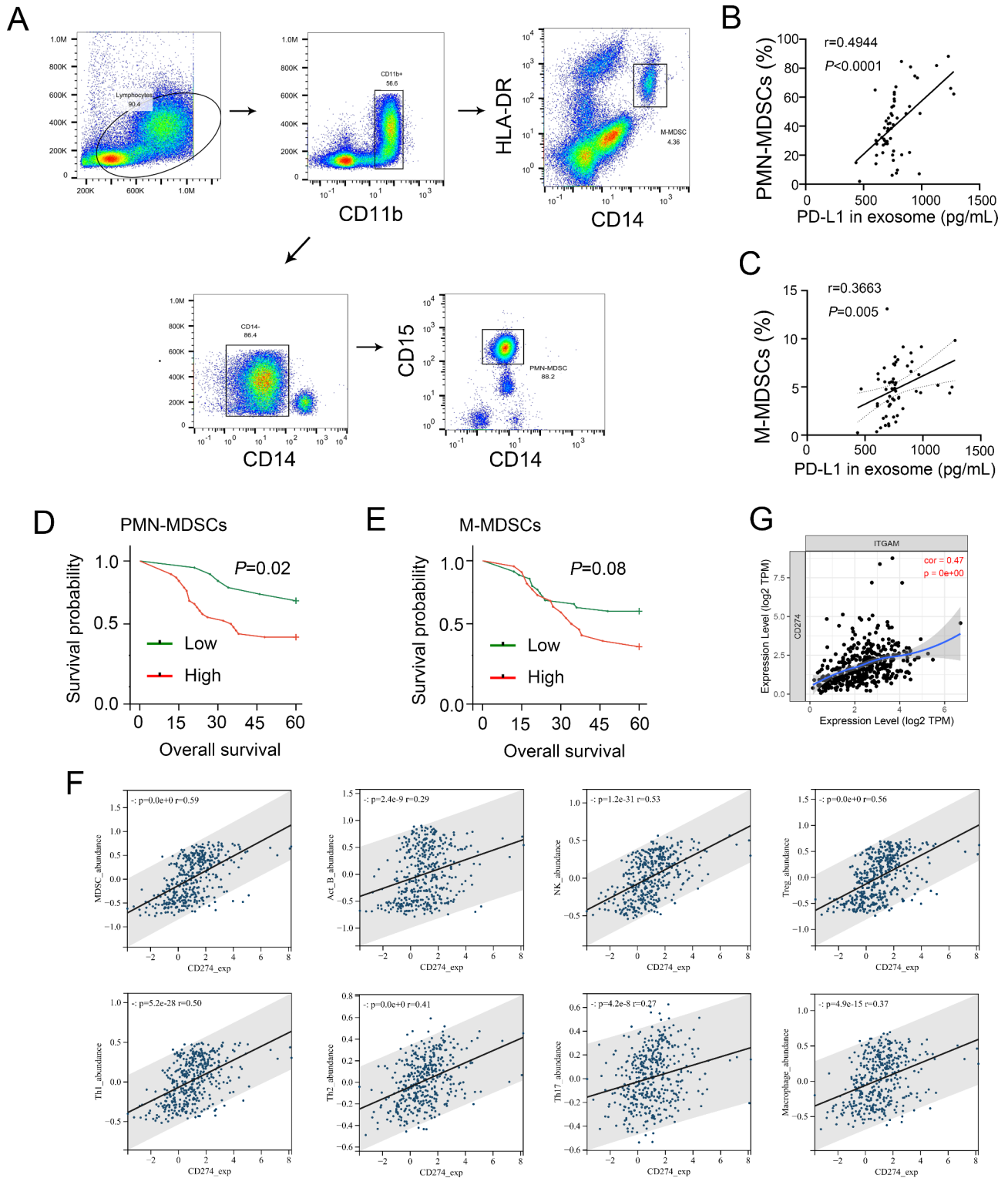
Fig. 3 Exosomal PD-L1 was strongly associated with the levels of MDSCs in GC patients. (**A**) MDSCs gating process in the peripheral blood of GC patients. (**B-C**) Correlation analysis between exosomal PD-L1 and PMN-/M-MDSCs. (**D-E**) Kaplan-Meier curves of OS of GC patients based on the PMN- and M-MDSCs frequencies. Graphics were made by an online website Sangerbox. (**F**) Correlation of PD-L1 expression with infiltrating levels of immune cells of GC tissues in TISIDB database. (**G**) Correlation of PD-L1 expression with CD11b (ITGAM) in TIMER database
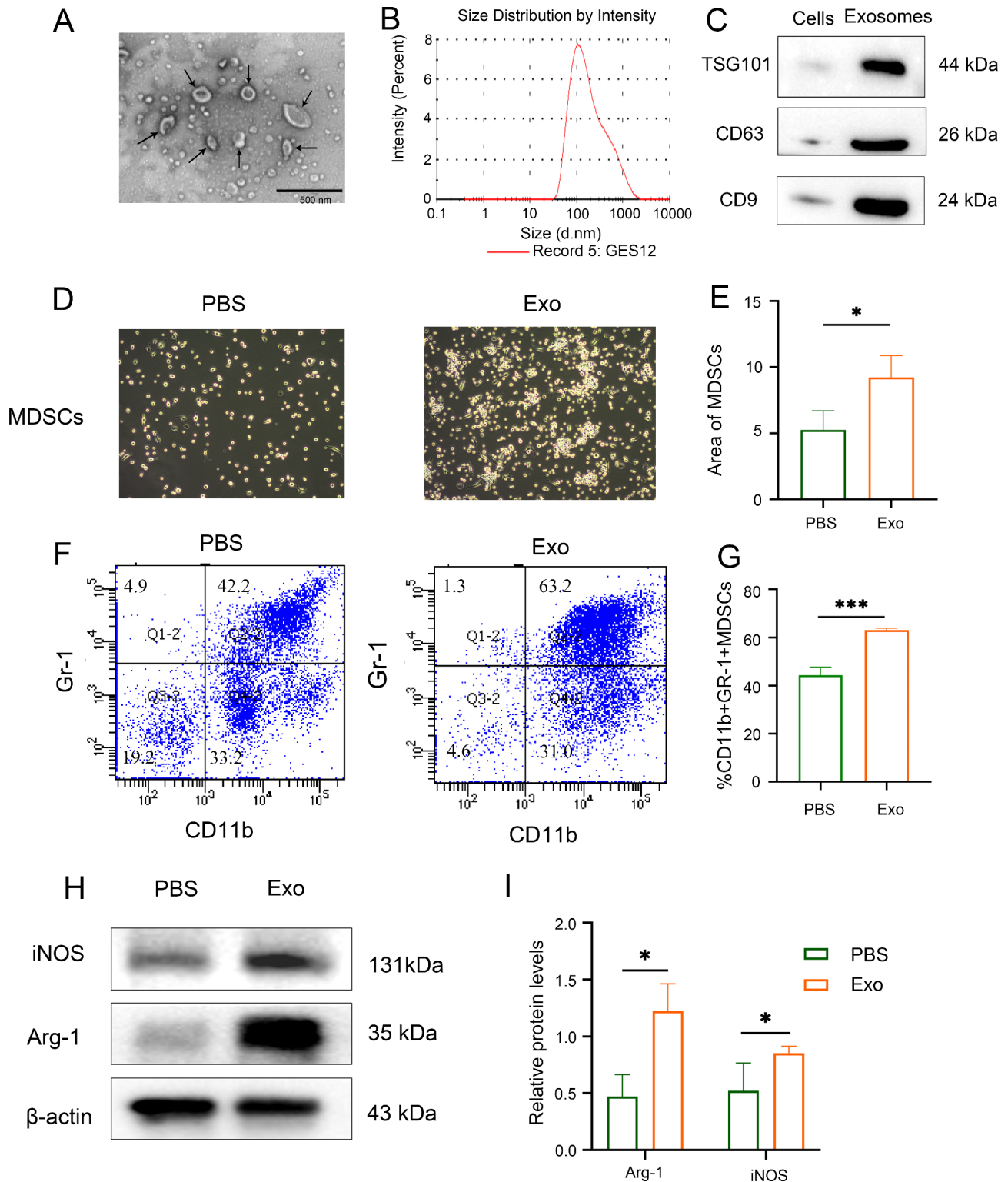
Fig. 4 Gastric cancer cell-derived exosomes can promote the expansion and immunosuppression of MDSCs. (**A**) Transmission electron microscopy image of exosomes. (**B**) NTA analysis confirmed the exosomes. (**C**) Western blot of the exosome-related markers in GC cell-derived exosomes. (**D-E**) The represent images of MDSCs after PBS or exosome intervention. (**F-G**) Percentages of CD11b⁺Gr-1⁺ MDSCs detected by flow cytometry. (**H-I**) The expression levels of iNOS and Arg-1 in MDSCs after PBS or exosome intervention. Data are expressed as the mean ± SEM. *$P < 0.05$, ***$P < 0.001$

GC cells. Compared with the PBS group, exosomes significantly promoted the proliferation of MDSCs (Fig. 4D-E) ($P<0.05$), and the number of MDSCs (CD11b$^+$Gr-1$^+$) were significantly increased (Fig. 4F-G) ($P<0.001$). As the main immunosuppressive factors of MDSCs, iNOS and Arg-1 were detected by Western blot, the results showed that the expression of iNOS ($P<0.05$) and Arg-1 ($P<0.05$) were increased after exosomes intervention. (Fig. 4H-I). The above results implied that GC-derived exosomes induced the expansion of MDSCs and mediated their immunosuppressive properties.

Exosomal PD-L1 promoted MDSC expansion via activation of IL-6/STAT3 pathway

To further investigate the role of exosomal PD-L1 in MDSCs expansion, lentiviral GV493 vector was used to stably knockdown PD-L1 in MFC cells, respectively(Fig. 5A). The strong green fluorescence after lentivirus transfection was observed by fluorescence microscope (Fig. 5B). Western blotting veritified that PD-L1 expression was significantly decreased in MFC cells and exosomes ($P<0.001$, $P<0.01$; Fig. 5C-D). Subsequently, MDSCs were treated with exosomes, and we found that the expansion of MDSCs were increased significantly in PD-L1-NC-Exo group ($P<0.001$) compared with PBS group and were significantly diminished
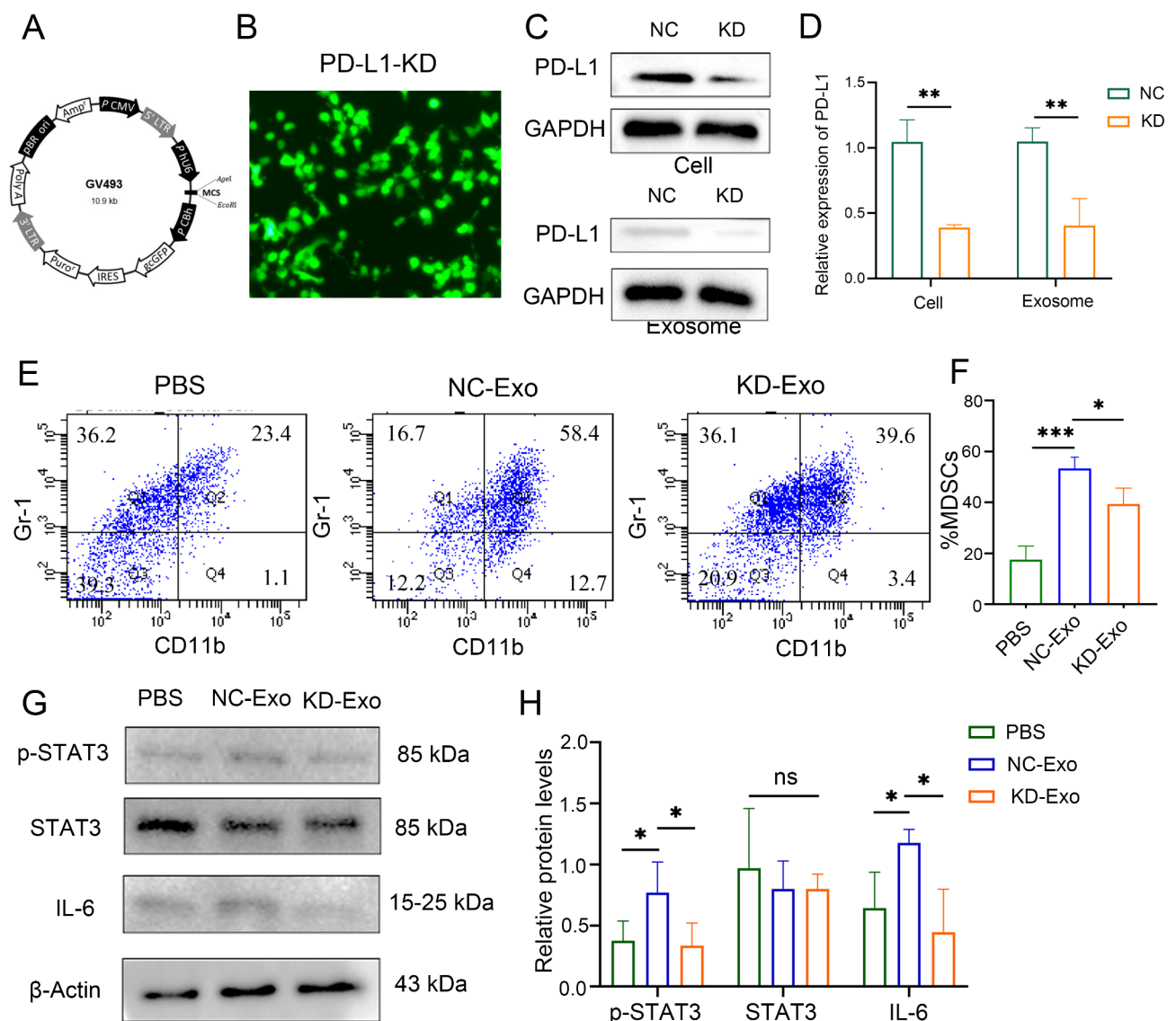

Fig. 5 Exosomal PD-L1 increased the MDSCs expansion through IL-6/STAT3 signaling pathway. (**A**) Lentivirus transfection of MFC cell lines. (**B**) Fluorescence images of PD-L1 after lentivirus transfection of MFC cells. (**C-D**) Western blotting analysis of the PD-L1 content in GC cells and exosome from the culture supernatant of GC cells. (**E-F**) Percentages of CD11b$^+$Gr-1$^+$MDSCs detected by flow cytometry. (**G-H**) Western blotting analysis of proteins in the IL-6/STAT3 signaling pathway. Data are expressed as the mean ± SEM. *$P<0.05$, ***$P<0.001$

in PD-L1-KD-Exo group ($P < 0.05$) compared with PD-L1-NC-Exo group (Fig. 5E-F).

It has been reported that the IL6-STAT3-DNMT1/3b epigenetic pathway silences the TNFα-RIP1 necrosis pathway to increase the survival rate of MDSC, thereby maintaining the accumulation of MDSC in tumor-bearing hosts [30], which led us to speculate that the expansion of MDSCs might also be related to the IL-6/STAT3 signaling pathway. Western blotting results showed that the expression of IL-6 ($P < 0.05$) and p-STAT3 ($P < 0.05$) was increased significantly in the PD-L1-NC-Exo group compared with PBS group, and was decreased significantly in the PD-L1-KD-Exo group ($P < 0.05$) compared with PD-L1-NC-Exo group (Fig. 5G-H). The above results implied that GC-derived exosomes induced the expansion of MDSCs might be mediated by exosomal PD-L1 through IL-6/STAT3 signaling pathway.

Exosomal PD-L1 promoted MDSCs expansion in GC cells-derived xenograft model

To further validate that the exosomal PD-L1 promoted MDSCs expansion, the experiments were next applied *in vivo*. The tumor weight in PD-L1-NC-Exo group ($P < 0.001$) was significantly higher compared with PBS group, and was decreased significantly in PD-L1-KD-Exo ($P < 0.001$) compared with PD-L1-NC-Exo group(Fig. 6A-B). Immunofluorescence results showed that the levels of PD-L1 in the intratumoral content of MDSCs (CD11b$^+$Gr-1$^+$) in PD-L1-NC-Exo group were higher compared with the PBS group, and were decreased in PD-L1-KD-Exo group compared with PD-L1-NC-Exo group (Fig. 6D). Moreover, flow cytometry analysis also showed the frequency of MDSCs (CD45$^+$CD11b$^+$Gr-1$^+$) was significantly increased in PD-L1-NC-Exo group ($P < 0.01$) compared with the PBS group, and were significantly decreased ($P < 0.05$) in PD-L1-KD-Exo group compared with PD-L1-NC-Exo group (Fig. 6E-F). Furthermore, it was found that the proportion of PD-L1$^+$MDSCs (PD-L1$^+$CD45$^+$CD11b$^+$Gr-1$^+$) was significantly increased in PD-L1-NC-Exo group ($P < 0.01$) compared with the PBS group, and were significantly decreased ($P < 0.05$) in PD-L1-KD-Exo group compared with PD-L1-NC-Exo group (Fig. 6E, G). The same phenomenon was observed in the spleen of mice (Fig. S2). Altogether, it was confirmed that exosomal PD-L1 might remodel the tumor microenvironment (TME) by promoting MDSCs expansion and finally enhanced tumor growth.

Discussion

For many years, cancer has been the main threat facing humanity. Many factors contribute to the occurrence of cancer, such as social modernization [31], and the use of chiral pesticides, pollutants, and drugs [5, 9, 32]. In 2017, the PD-1 inhibitor pembrolizumab was approved by the FDA for the treatment of recurrent locally advanced or metastatic stomach or adenocarcinoma of the esophagogastric junction that expresses PD-L1 [33]. Because most GC patients are insensitive to immune checkpoints (ICIs) [34, 35]. Immune checkpoint blockade (ICB) has achieved important therapeutic effects in many cancers, but its clinical activity is limited to some patients [35]. Therefore, it is particularly important to have a deeper understanding of the role of PD-L1 in ICB treatment.

Over the past decade, an increasing body of research has demonstrated that exosomes can induce pleiotropic functional responses in recipient cells, leading to various health complications such as cancer, neurodegenerative illnesses, rheumatic diseases, and infectious diseases [21, 36–38]. Exosomal miR-200a is related to EMT-mediated GC metastasis [20]. As a type of small secreted membrane vesicles, TDEs played a crucial role in the development of tumors, particularly in controlling the immune response associated with the tumor [39, 40]. Many proteins and nucleic acid molecules in TDEs could serve as markers in monitoring the therapeutic responses in cancer patients [41, 42]. PD-L1 was found in microvesicles, and exosomal PD-L1 had the same membrane topology with the cell surface PD-L1, with its extracellular domain exposed on the surface [24], which indicated that PD-L1 in TDEs could be a potential target to develop a novel clinical therapeutic strategy to tumors.

It had been demonstrated that the development, differentiation, and accumulation of MDSCs in multiple tumor [43]. MDSCs are distinguished by their capacity to impede T-cell proliferation and function via multiple mechanisms, including the expression of NADPH oxidase (Nox2), arginase 1 (Arg-1), oxide synthase 2 (Nos2), and S100A8/9, which permit tumor cells to evade immune system attack [43]. Myeloid precursor cells' development into MDSCs could be skewed by TDEs [44, 45]. Macrophage migration inhibitory factor (MIF) in both human and murine pancreatic cancer-derived exosomes was reported to have the key role in inducing MDSC formation in pancreatic cancer [46]. Inhibition of the IL-6/STAT3 pathway can alleviate immunosuppression caused by MDSCs [47]. Nevertheless, the cell-cell communication between GC cells and MDSCs mediated by exosomes was not clear. Our study provided ideas for the interaction between exosomes and MDSC in TME.

Circulating soluble PD-L1 was easy to measure in GC patients, and its level was related to the expression of PD-L1 in GC tissues, inflammatory cell infiltration and disease progression [48]. In addition, it was reported that PD-L1 was also enriched in exosomes, which might prevent T cells from killing one another in order to maintain its immunosuppressive effects in the GC microenvironment [49]. It could also induce the higher levels of T-cell dysfunction due to its higher stability
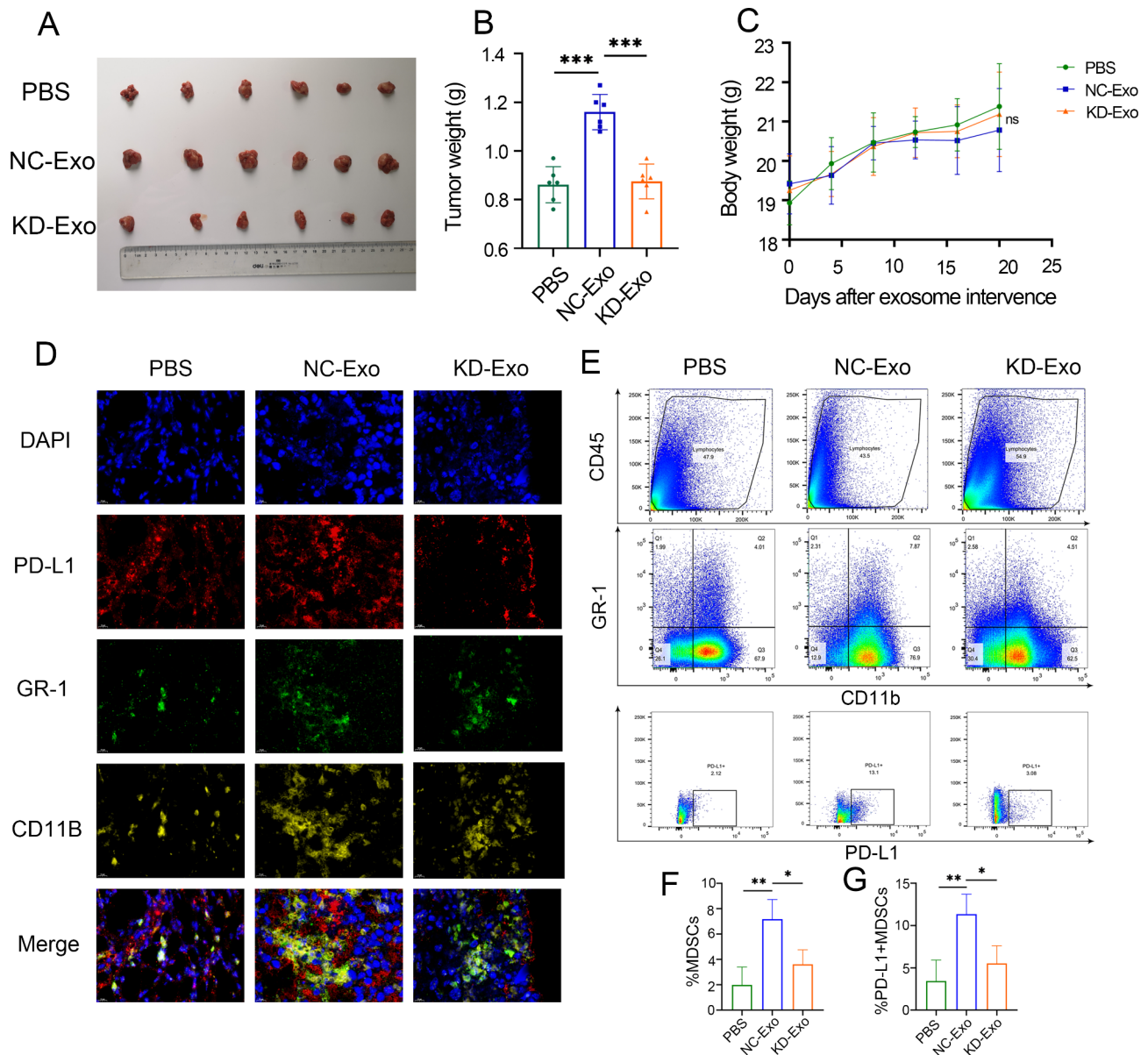
Fig. 6 Exosomal PD-L1 promoted MDSC expansion in vivo. (**A**) Representative images of xenograft tumors in mice implanted with MFC cells and receiving PBS, NC-PD-L1-exosome or KD-PD-L1- exosomes treatment (*n* = 6/group). (**B**) The tumor weights at the last measurement. (**C**) The body weights were measured every 4 days. (**D**) Immunofluorescence staining for DAPI (nucleus), CD11b, Gr-1, and PD-L1 in tumor tissue sections from the xenograft tumor model. (**E-G**) Percentages of MDSCs (CD45⁺CD11b⁺gr1⁺) and PD-L1⁺MDSCs in tumors determined via flow cytometry. The significance of the difference was tested with one-way ANOVA. *$P < 0.05$, **$P < 0.01$, ***$P < 0.001$, ns: not significant

and MHC I expression in GC [50]. To systemically combat anti-tumor immunity, melanoma cells could release PD-L1-positive extracellular vesicles into the tumor microenvironment and circulation [24]. Genetically blocking exosome biogenesis or deleting Pd-l1 reverses the phenotype by strongly promoting T cells activation, proliferation, and killing potential [51]. Here, through bioinformatic analysis, we found that exosomal PD-L1 existed in the peripheral blood was correlated with poor prognosis of GC patients. We further revealed that exosomal PD-L1 was higher in AJCC stage III and IV but not

in AJCC stage I and II and was related to the poor prognosis of GC patients. The above results indicated that as a molecular marker, exosomal PD-L1 could predict the survival of GC patients, which might be mediated by inducing the expansion of MDSCs. However, the interaction between exosomal PD-L1 and MDSCs in the tumor microenvironment remains to be explored. In this study, we discovered that the high MDSC numbers could be induced by GC cell-derived exosome. Subsequent investigation revealed a strong correlation between PD-L1 existed in exosomal forms and tumor-infiltrating MDSC

in STAD as well as the number of MDSCs in the peripheral blood of GC patients.

The IL-6/STAT3 signaling pathway was shown to be one of the critical pathways in mediating the expansion of MDSCs [26]. Blocking of IL-6 function mostly inhibited STAT3 phosphorylation and the MDSCs expansion in BM cells [26]. However, the mechanism of exosomes promoting MDSC proliferation still needs to be explored. In vitro study, we found that exosomes facilitated expansion of MDSCs through promoting the expression of IL-6 and activating STAT3 phosphorylation, while the expression of IL-6/p-STAT3 and the accumulation of MDSCs were inhibited when the exosomal PD-L1 was decreased. Next, exosomal PD-L1 was discovered to encourage MDSCs development both in vitro and in vivo and quicken tumor growth, suggesting that exosomal PD-L1 promoted tumor growth most likely by stimulating MDSC expansion. These results provided a evidence for immunosuppressive effects of MDSCs in GC.

Conclusion

In summary, we found that the higher levels of exosomal PD-L1 is related to poor prognosis for GC patients. Exosomal PD-L1 were also found to promote tumor growth and induce expansion of MDSCs though IL-6/STAT3 signaling in vivo and vitro experiments. These findings show that exosomal PD-L1 has the potential to become a prognostic and diagnostic biomarker for GC patients and provide a new strategy for immunotherapy of GC using exosomal PD-L1 as a target.

Abbreviations

MDSCs	Myeloid-derived suppressor cells
GC	Gastric cancer
TDEs	Tumor-derived exosomes
ELISA	Enzyme-linked immunosorbent test
TEM	Transmission electron microscopy
CDX	Cells-derived xenograft
Nox2	NADPH oxidase
Arg-1	Arginase 1
Nos2	NADPH oxide synthase 2
ICIs	Immune Checkpoints
MVB	Multivesicular bodies
MIF	Macrophage migration inhibitory factor

Supplementary Information

The online version contains supplementary material available at https://doi.org/10.1186/s12967-024-05611-y.

Supplementary Material 1

Data availability
All data generated or analyzed during this study are included in this published article.

Declarations

Ethics approval and consent to participate
All clinical experiments were approved by the Independent Ethics Committee of the Affiliated Hospital of Nanjing University of Chinese Medicine, Number: 2021NL-133-03. All patients were informed based on approved ethical guidelines, and patients who agreed to participate in this study signed consent forms before being included in the study. We also confirmed that all methods were performed in accordance with the relevant guidelines and regulations. All studies were conducted in accordance with the principles of the Declaration of Helsinki.

Consent for publication
Not applicable.

Competing interests
The authors declare that they have no known competing financial interests or personal relationships that could have appeared to influence the work reported in this paper.

Author details
[1] Jiangsu Province Key Laboratory of Tumor Systems Biology and Chinese Medicine, Jiangsu Province Hospital of Chinese Medicine, Affiliated Hospital of Nanjing University of Chinese Medicine, 155 Hanzhong Road, Nanjing 210029, Jiangsu, China
[2] No.1 Clinical Medical College, Nanjing University of Chinese Medicine, Nanjing 210023, Jiangsu, China
[3] Department of General Surgery, Yixing Traditional Chinese Medicine Hospital, Wuxi 214200, Jiangsu, China

References
1. Sung H, Ferlay J, Siegel RL, Laversanne M, Soerjomataram I, Jemal A, Bray F. Global Cancer statistics 2020: GLOBOCAN estimates of incidence and Mortality Worldwide for 36 cancers in 185 countries. CA Cancer J Clin. 2021;71:209–49.
2. Herrero R, Parsonnet J, Greenberg ER. Prevention of gastric cancer. JAMA. 2014;312:1197–8.
3. Kang YK, Boku N, Satoh T, Ryu MH, Chao Y, Kato K, Chung HC, Chen JS, Muro K, Kang WK, et al. Nivolumab in patients with advanced gastric or gastrooesophageal junction cancer refractory to, or intolerant of, at least two previous chemotherapy regimens (ONO-4538-12, ATTRACTION-2): a randomised, double-blind, placebo-controlled, phase 3 trial. Lancet. 2017;390:2461–71.
4. Kang YK, Chen LT, Ryu MH, Oh DY, Oh SC, Chung HC, Lee KW, Omori T, Shitara K, Sakuramoto S, et al. Nivolumab plus chemotherapy versus placebo plus chemotherapy in patients with HER2-negative, untreated, unresectable advanced or recurrent gastric or gastro-oesophageal junction cancer

(ATTRACTION-4): a randomised, multicentre, double-blind, placebo-controlled, phase 3 trial. Lancet Oncol. 2022;23:234–47.

5. Ali I, Wani WA, Haque A, Saleem K. Glutamic acid and its derivatives: candidates for rational design of anticancer drugs. Future Med Chem. 2013;5:961–78.

6. Ali I, Wani WA, Saleem K, Wesselinova D. Syntheses, DNA binding and anti-cancer profiles of L-glutamic acid ligand and its copper(II) and ruthenium(III) complexes. Med Chem. 2013;9:11–21.

7. Ali I, Waseem AW, Saleem K, Haque A. Thalidomide: a banned drug resurged into Future Anticancer Drug. Curr Drug Therapy. 2012;7:13–23.

8. Ali I, Alsehli M, Scotti L, Tullius Scotti M, Tsai ST, Yu RS, Hsieh MF, Chen JC. Progress in Polymeric Nano-Medicines for Theranostic Cancer Treatment. Polym (Basel) 2020, 12.

9. Ali I, Wani WA, Khan A, Haque A, Ahmad A, Saleem K, Manzoor N. Synthesis and synergistic antifungal activities of a pyrazoline based ligand and its copper(II) and nickel(II) complexes with conventional antifungals. Microb Pathog. 2012;53:66–73.

10. Huseni MA, Wang L, Klementowicz JE, Yuen K, Breart B, Orr C, Liu LF, Li Y, Gupta V, Li C, et al. CD8(+) T cell-intrinsic IL-6 signaling promotes resistance to anti-PD-L1 immunotherapy. Cell Rep Med. 2023;4:100878.

11. Ma Z, Sun Q, Zhang C, Zheng Q, Liu Y, Xu H, He Y, Yao C, Chen J, Xia H. RHOJ induces epithelial-to-mesenchymal transition by IL-6/STAT3 to Promote Invasion and Metastasis in Gastric Cancer. Int J Biol Sci. 2023;19:4411–26.

12. Lu G, Tian S, Sun Y, Dong J, Wang N, Zeng J, Nie Y, Wu K, Han Y, Feng B, Shang Y. NEK9, a novel effector of IL-6/STAT3, regulates metastasis of gastric cancer by targeting ARHGEF2 phosphorylation. Theranostics. 2021;11:2460–74.

13. de Visser KE, Joyce JA. The evolving tumor microenvironment: from cancer initiation to metastatic outgrowth. Cancer Cell. 2023;41:374–403.

14. Xiao Y, Yu D. Tumor microenvironment as a therapeutic target in cancer. Pharmacol Ther. 2021;221:107753.

15. Liu Y, Li C, Lu Y, Liu C, Yang W. Tumor microenvironment-mediated immune tolerance in development and treatment of gastric cancer. Front Immunol. 2022;13:1016817.

16. Yasuda T, Wang YA. Gastric cancer immunosuppressive microenvironment heterogeneity: implications for therapy development. Trends Cancer. 2024;10:627–42.

17. Kim W, Chu TH, Nienhüser H, Jiang Z, Del Portillo A, Remotti HE, White RA, Hayakawa Y, Tomita H, Fox JG, et al. PD-1 signaling promotes tumor-infiltrating myeloid-derived suppressor cells and gastric tumorigenesis in mice. Gastroenterology. 2021;160:781–96.

18. Paskeh MDA, Entezari M, Mirzaei S, Zabolian A, Saleki H, Naghdi MJ, Sabet S, Khoshbakht MA, Hashemi M, Hushmandi K, et al. Emerging role of exosomes in cancer progression and tumor microenvironment remodeling. J Hematol Oncol. 2022;15:83.

19. Ashrafizadeh M, Kumar AP, Aref AR, Zarrabi A, Mostafavi E. Exosomes as Promising nanostructures in Diabetes Mellitus: from insulin sensitivity to ameliorating Diabetic complications. Int J Nanomed. 2022;17:1229–53.

20. Mirzaei S, Gholami MH, Aghdaei HA, Hashemi M, Parivar K, Karamian A, Zarrabi A, Ashrafizadeh M, Lu J. Exosome-mediated miR-200a delivery into TGF-β-treated AGS cells abolished epithelial-mesenchymal transition with normalization of ZEB1, vimentin and Snail1 expression. Environ Res. 2023;231:116115.

21. Xu R, Rai A, Chen M, Suwakulsiri W, Greening DW, Simpson RJ. Extracellular vesicles in cancer - implications for future improvements in cancer care. Nat Rev Clin Oncol. 2018;15:617–38.

22. Frigola X, Inman BA, Lohse CM, Krco CJ, Cheville JC, Thompson RH, Leibovich B, Blute ML, Dong H, Kwon ED. Identification of a soluble form of B7-H1 that retains immunosuppressive activity and is associated with aggressive renal cell carcinoma. Clin Cancer Res. 2011;17:1915–23.

23. Ruffner MA, Kim SH, Bianco NR, Francisco LM, Sharpe AH, Robbins PD. B7-1/2, but not PD-L1/2 molecules, are required on IL-10-treated tolerogenic DC and DC-derived exosomes for in vivo function. Eur J Immunol. 2009;39:3084–90.

24. Chen G, Huang AC, Zhang W, Zhang G, Wu M, Xu W, Yu Z, Yang J, Wang B, Sun H, et al. Exosomal PD-L1 contributes to immunosuppression and is associated with anti-PD-1 response. Nature. 2018;560:382–6.

25. Yang Y, Li CW, Chan LC, Wei Y, Hsu JM, Xia W, Cha JH, Hou J, Hsu JL, Sun L, Hung MC. Exosomal PD-L1 harbors active defense function to suppress T cell killing of breast cancer cells and promote tumor growth. Cell Res. 2018;28:862–4.

26. Zhang X, Li F, Tang Y, Ren Q, Xiao B, Wan Y, Jiang S. miR-21a in exosomes from Lewis lung carcinoma cells accelerates tumor growth through targeting

27. PDCD4 to enhance expansion of myeloid-derived suppressor cells. Oncogene. 2020;39:6354–69.

27. Şahin F, Koçak P, Güneş MY, Özkan İ, Yıldırım E, Kala EY. In Vitro Wound Healing activity of wheat-derived nanovesicles. Appl Biochem Biotechnol. 2019;188:381–94.

28. Wu J, Yuan M, Shen J, Chen Y, Zhang R, Chen X, Wang H, Yin Z, Zhang X, Liu S, Sun Q. Effect of modified Jianpi Yangzheng on regulating content of PKM2 in gastric cancer cells-derived exosomes. Phytomedicine. 2022;103:154229.

29. Gabrilovich DI, Nagaraj S. Myeloid-derived suppressor cells as regulators of the immune system. Nat Rev Immunol. 2009;9:162–74.

30. Smith AD, Lu C, Payne D, Paschall AV, Klement JD, Redd PS, Ibrahim ML, Yang D, Han Q, Liu Z, et al. Autocrine IL6-Mediated activation of the STAT3-DNMT Axis silences the TNFα-RIP1 necroptosis pathway to Sustain Survival and Accumulation of myeloid-derived suppressor cells. Cancer Res. 2020;80:3145–56.

31. Ali I, Wani WA, Saleem K, Hsieh M-F. Anticancer metallodrugs of glutamic acid sulphonamides: DNA binding, hemolysis and anticancer studies. RSC Adv. 2014;4:29629–41.

32. Ali I, Aboul-Enein HY, Ghanem A. Enantioselective toxicity and carcinogenesis. Curr Pharm Anal. 2005;1:109–25.

33. Fashoyin-Aje L, Donoghue M, Chen H, He K, Veeraraghavan J, Goldberg KB, Keegan P, McKee AE, Pazdur R. FDA approval Summary: Pembrolizumab for recurrent locally Advanced or metastatic gastric or gastroesophageal Junction Adenocarcinoma expressing PD-L1. Oncologist. 2019;24:103–9.

34. Kono K, Nakajima S, Mimura K. Current status of immune checkpoint inhibitors for gastric cancer. Gastric Cancer. 2020;23:565–78.

35. Topalian SL, Hodi FS, Brahmer JR, Gettinger SN, Smith DC, McDermott DF, Powderly JD, Carvajal RD, Sosman JA, Atkins MB, et al. Safety, activity, and immune correlates of anti-PD-1 antibody in cancer. N Engl J Med. 2012;366:2443–54.

36. Howitt J, Hill AF. Exosomes in the Pathology of neurodegenerative diseases. J Biol Chem. 2016;291:26589–97.

37. Beyer C, Pisetsky DS. The role of microparticles in the pathogenesis of rheumatic diseases. Nat Rev Rheumatol. 2010;6:21–9.

38. Schorey JS, Harding CV. Extracellular vesicles and infectious diseases: new complexity to an old story. J Clin Invest. 2016;126:1181–9.

39. Hingorani SR. Intercepting Cancer communiques: Exosomes as Heralds of Malignancy. Cancer Cell. 2015;28:151–3.

40. Steinbichler TB, Dudás J, Riechelmann H, Skvortsova II. The role of exosomes in cancer metastasis. Semin Cancer Biol. 2017;44:170–81.

41. An T, Qin S, Xu Y, Tang Y, Huang Y, Situ B, Inal JM, Zheng L. Exosomes serve as tumour markers for personalized diagnostics owing to their important role in cancer metastasis. J Extracell Vesicles. 2015;4:27522.

42. Gold B, Cankovic M, Furtado LV, Meier F, Gocke CD. Do circulating tumor cells, exosomes, and circulating tumor nucleic acids have clinical utility? A report of the association for molecular pathology. J Mol Diagn. 2015;17:209–24.

43. Kumar V, Patel S, Tcyganov E, Gabrilovich DI. The nature of myeloid-derived suppressor cells in the Tumor Microenvironment. Trends Immunol. 2016;37:208–20.

44. Guo X, Qiu W, Wang J, Liu Q, Qian M, Wang S, Zhang Z, Gao X, Chen Z, Guo Q, et al. Glioma exosomes mediate the expansion and function of myeloid-derived suppressor cells through microRNA-29a/Hbp1 and microRNA-92a/Prkar1a pathways. Int J Cancer. 2019;144:3111–26.

45. Guo X, Qiu W, Liu Q, Qian M, Wang S, Zhang Z, Gao X, Chen Z, Xue H, Li G. Immunosuppressive effects of hypoxia-induced glioma exosomes through myeloid-derived suppressor cells via the miR-10a/Rora and miR-21/Pten pathways. Oncogene. 2018;37:4239–59.

46. Jia X, Xi J, Tian B, Zhang Y, Wang Z, Wang F, Li Z, Long J, Wang J, Fan GH, Li Q. The tautomerase activity of Tumor Exosomal MIF promotes pancreatic Cancer Progression by modulating MDSC differentiation. Cancer Immunol Res. 2024;12:72–90.

47. Neo SY, Tong L, Chong J, Liu Y, Jing X, Oliveira MMS, Chen Y, Chen Z, Lee K, Burduli N, et al. Tumor-associated NK cells drive MDSC-mediated tumor immune tolerance through the IL-6/STAT3 axis. Sci Transl Med. 2024;16:eadi2952.

48. Chivu-Economescu M, Herlea V, Dima S, Sorop A, Pechianu C, Procop A, Kitahara S, Necula L, Matei L, Dragu D, et al. Soluble PD-L1 as a diagnostic and prognostic biomarker in resectable gastric cancer patients. Gastric Cancer. 2023;26:934–46.

49. Shen DD, Pang JR, Bi YP, Zhao LF, Li YR, Zhao LJ, Gao Y, Wang B, Wang N, Wei L, et al. LSD1 deletion decreases exosomal PD-L1 and restores T-cell response in gastric cancer. Mol Cancer. 2022;21:75.

50. Fan Y, Che X, Qu J, Hou K, Wen T, Li Z, Li C, Wang S, Xu L, Liu Y, Qu X. Exosomal PD-L1 retains immunosuppressive activity and is Associated with gastric Cancer prognosis. Ann Surg Oncol. 2019;26:3745–55.

51. Poggio M, Hu T, Pai CC, Chu B, Belair CD, Chang A, Montabana E, Lang UE, Fu Q, Fong L, Blelloch R. Suppression of exosomal PD-L1 induces systemic anti-tumor immunity and memory. Cell. 2019;177:414–e427413.

Publisher's note